Lateral Variations of *P*-Wave Velocity from Deep Borehole Data in the Southern Apennines, Italy

Paola Montone[1] and Maria Teresa Mariucci[1]

Abstract—We have selected 28 deep wells in the Southern Apennine area, most of which are located along and around the Val d'Agri Basin. The Southern Apennines, one of the most seismically active regions of the Italian peninsula, is a NE-verging fold-and-thrust belt characterised by the Meso–Cenozoic Apulia carbonate duplex system overlain by a thick column of Apennine carbonate platform and Lagonegro basin units. These units are unconformably covered by Neogene siliciclastic successions. Among the many Quaternary tectonic basins in the area, the Val d'Agri Basin is the most important intramontane depression, and is bordered by a ∼ NW–SE-trending active fault system that represents one of the main seismogenic structures of the region. Moreover, the Val d'Agri Basin is the largest onshore oil field basin in Europe. In this context, we have analysed sonic log records from 28 deep wells and compared them with the corresponding stratigraphy and the other geophysical logs. We have obtained detailed measurements of the *P*-wave velocity (*Vp*) for each well from 0 to ∼ 6 km depth, and found important lateral variations of *Vp* over very small distances. From these values, we have retrieved the densities of the main units crossed by the wells and the range of the overburden gradient in this area.

Keywords: Deep boreholes, sonic log, *Vp* value, crustal structure, Southern Italy.

1. Introduction

We have performed this study in southern Italy (Fig. 1) between the Campania, Basilicata, and Apulia regions for two main reasons: (1) the Southern Apennines are one of the most hazardous regions in Italy and in the Mediterranean area (Rovida et al., 2022), and (2) the Val D'Agri Basin is the largest oil field in onshore Europe (Van Dijk et al., 2000b).

To define the *Vp* crustal velocity between 0 and ∼ 6 km depth, we analysed 28 deep wells available to us, located in the Southern Apennines that is formed by the Apennine carbonate platform at west, the Lagonegro basin, the inner Apulian carbonate platform and Quaternary basins (Fig. 2). In detail 22 of these wells are located along and around the Val d'Agri Basin, an oil field drilled at depths 2 to 3 km below sea level, with the reservoir hosted in the Apulia platform, sealed at the top by flysch and mélange sequences (Shiner et al., 2004; Van Dijk et al., 2000b). Only seven of the 28 wells are public (nos. 1, 2, 3, 4, 26, 27, and 28); their data can be found in the database of the National Mining Office for Hydrocarbon and Geothermal Energy (UNMIG) of the Italian Ministry of the Environment. In the Videpi archive (https://www.videpi.com) stratigraphic logs of wells can be viewed and downloaded, typically associated with geophysical logs.

We have analysed the sonic curves of geophysical log records for deep wells drilled by major oil companies and compared them with the stratigraphy of each well and with other geophysical records, such as resistivity and gamma ray logs.

First, we have grouped the wells based on their geographical locations, identifying them with different colours (Fig. 2); different shades of the same colour (e.g. green) indicate neighbouring wells that could also belong to the same group. The 28 deep wells were drilled in sedimentary rocks, mainly Meso–Cenozoic calcareous and siliciclastic successions, Miocene–Pliocene arenaceous-clayey terrigenous flysch, and Quaternary deposits. Wells 1 to 4 are in the north and westernmost parts of the study area; wells 2 and 4 belong to the Apennine carbonate platform domain, whereas well 1 and 3,
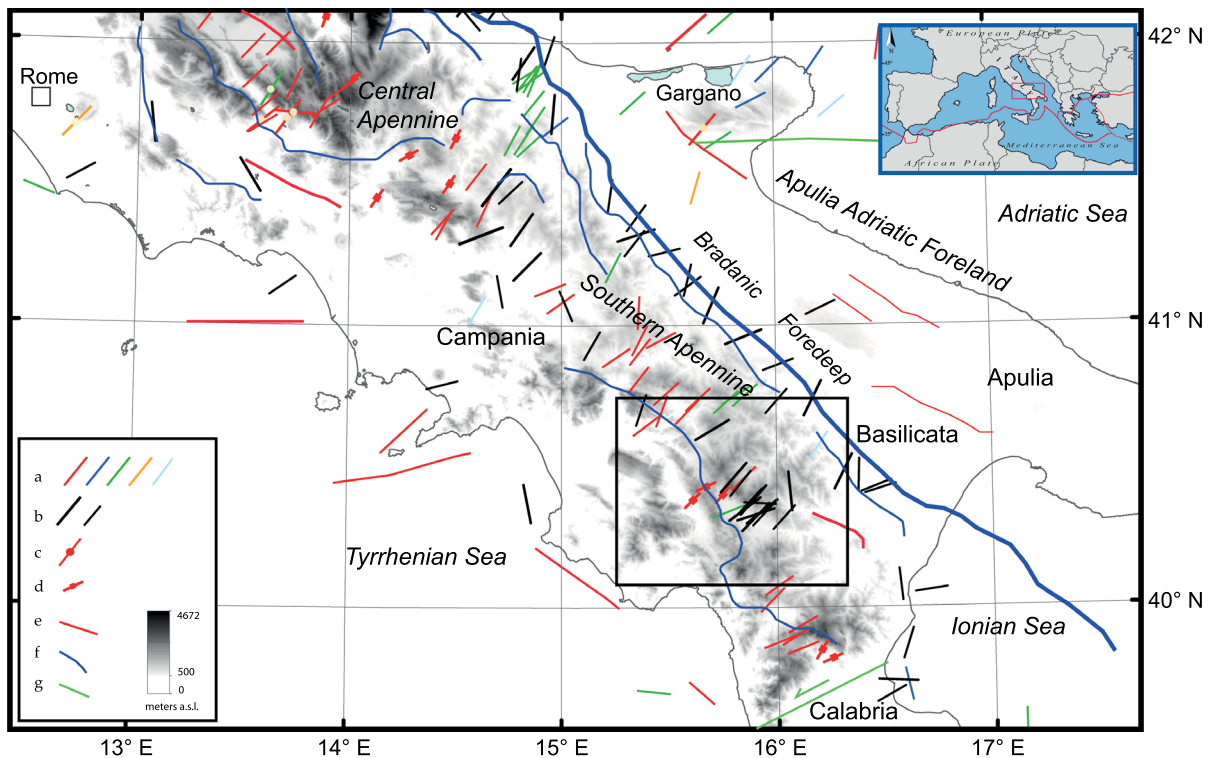
Figure 1

Main tectonic features of southern Italy, modified after Vezzani et al. (2010). Minimum horizontal stress directions from the Italian Present-day Stress Indicators database, IPSI 1.5 (Mariucci & Montone, 2022). minimum horizontal stress orientations from: **a** earthquake focal mechanisms with M > 4.0 (red: normal faulting; blue: thrusting; green: strike slip; orange: normal strike; light blue: thrust strike); **b** borehole breakout data (larger symbols indicate better quality results than the smaller ones); **c** formal inversion of earthquake focal mechanisms; **d** fault data. Tectonics: **e** normal faults; **f** thrust faults; **g** strike-slip faults. For detailed explanations of present-day stress indicators, see Montone & Mariucci (2016). The map has been generated with Esri ArcGIS Desktop 10.2 (http://www.esri.com). Box represents the area of Fig. 2

together with wells 5, 6, 12, 13, 14, and 27, are located within the Lagonegro basin succession. Wells 21 to 25 are located within the Val d'Agri Basin, and the remaining wells, found farther east and south (well 28), are located within the Miocene–Pliocene terrigenous deposits (Fig. 2). The maximum depth of the wells is 6200 m, and the minimum is 3070 m; on average, the wells are 4000–5000 m deep. Most are nearly vertical wells, but several have maximum vertical inclinations of about 30°; three of the 28 wells have horizontal portions that we have not taken into account.

The obtained results are in terms of *P*-wave velocity values with respect to the main tectono-stratigraphic units crossed by the wells. By applying an appropriate formula for the sedimentary rocks, we have also retrieved the respective density values

(Gardner et al., 1974). These results have allowed us to estimate the lithostatic gradient, which in this area increases from the easternmost boreholes, closest to the Bradanic foredeep, to the innermost wells in the Apennine belt. The *P*-wave velocities observed show a great variability over a distance of $\sim$ 50 to 60 km. We have assigned reference *Vp* and density values to each tectono-stratigraphic unit crossed by the wells, and computed the median *Vp* and density values of the empirical cumulative distribution by length and the 10th–90th percentiles as the variability range, as well as the means weighted by length with standard deviations for comparison.

Recently, a revision of the 3D seismic volume for the Val d'Agri Basin was published based on geological information and seismic data processing, which were used to estimate static corrections for
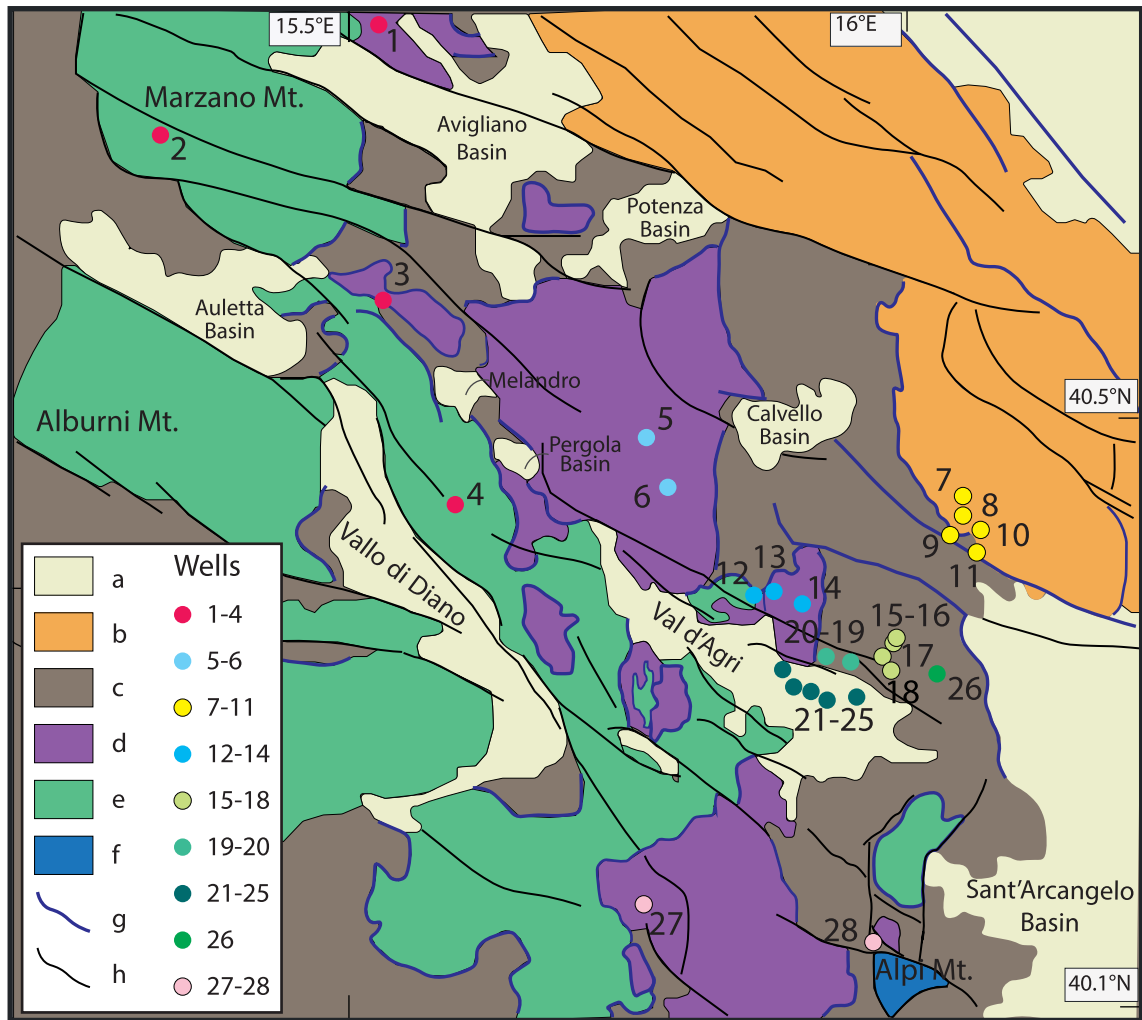
Figure 2
Geological and tectonic scheme of the study area modified after Catalano et al. (2004) and Improta et al. (2017). Locations of 28 analysed deep boreholes. Legend: **a** Quaternary continental deposits, corresponding to Q; **b** flysch and terrigenous sediments of satellite basins (middle Miocene–Pliocene), partially corresponding to ACT; **c** pelagic and slope successions, mainly clays and slope carbonates (Cretaceous–lower Miocene), partially corresponding to FLY; **d** Lagonegro basin, mainly cherty limestones, cherts, and claystones (Mesozoic), corresponding to LAG; **e** Apennine carbonate platform (Mesozoic), corresponding to APP; **f** Apulia platform (Mesozoic–Miocene), corresponding to PAI; **g** main reverse faults and overthrusts; **h** normal faults. Wells: different colours indicate different geological and geographical location. See further details in the text

data preconditioning before imaging, and to build the velocity model for depth imaging (Pajola et al., 2020). The *Vp* values of some "main stratigraphic zones" defined in that paper allow for comparison with our results. In general, we observe lower *P*-velocities relative to those obtained by their analysis, which could be due to the different methods used, as discussed below.

Intense structural complexity of the region was also imaged by the local tomography, where first-order lateral *Vp* variations were related to rapid depth changes of deeper carbonate successions (Improta et al., 2017; Valoroso et al., 2011).

In central Italy, destructive earthquakes have occurred within the last 25 years, including the 1997 Colfiorito (e.g. Amato et al., 1998; Boncio & Lavecchia, 2000; Calamita et al., 2000; Chiarabba &

Amato, 2003; Cinti et al., 2000; Ekstrom et al., 1998), 2009 L'Aquila (e.g. Di Stefano et al., 2011; Walters et al., 2009), and 2016–2018 Amatrice–Norcia seismic sequences (e.g. Chiaraluce et al., 2017; Tinti et al., 2016). Recently calculated Vp values in this area (Mariucci & Montone, 2016; Montone & Mariucci, 2020; Trippetta et al., 2021) allowed better definition of the seismic velocities of the shallow crust, increased knowledge of the subsurface, and improved geophysical models (Barchi et al., 2021; Buttinelli et al., 2021), which we also expect to achieve using the results of this study.

2. Geological Framework and Seismicity

The selected study area is in the Southern Apennines, a typical fold-and-thrust belt with eastern to north-eastern vergence (e.g. see Royden et al., 1987) located between the Tyrrhenian back-arc basin to the west and the Bradanic foredeep and Apulia Adriatic foreland to the east (Fig. 1).

The fold-and-thrust belt consists of Mesozoic–Tertiary shallow-water carbonate platform and Lagonegro basin pelagic successions of the Adria passive margin (Patacca & Scandone, 1989). These units were completely detached from their original substratum and moved onto the inner Apulia platform foreland sequence (e.g. Doglioni et al., 1996; Improta et al., 2017; Mazzoli et al., 2004; Menardi Noguera & Rea, 2000). The buried Apulia platform comprises a thickness of about 6–8 km of predominantly Jurassic to Miocene carbonate rocks, with Triassic evaporites at the base. It is characterised by double verging anticlines bounded by high-angle reverse faults (Casero, 2004). Only in the Monte Alpi tectonic window (Fig. 2) does the inner Apulia carbonate system outcrop at about 2000 m above sea level, whereas the autochthonous portion of the Apulia platform crops out more to the east along the foreland (Patacca & Scandone, 2004). The Apulia platform carbonates are stratigraphically covered by late Miocene–Pliocene marine sediments, which act as a seal of unlocked hydrocarbon traps (Casero, 2004; Roure et al., 2012). The entire succession ends with the unconformity overlain by Pliocene–Pleistocene foredeep deposits.

The current structural setting of the Southern Apennine belt is the result of compressive and extensional tectonic events associated with the subduction and subsequent flexural retreat of the Adriatic plate and, starting from the Tortonian, with the opening of the Tyrrhenian retroback-arc basin. Beginning in the Early Pliocene, the Southern Apennine accretionary wedge was thrusted over the western margin of the Apulia platform; during the Late Pliocene-Early Pleistocene final compressional phases, this platform was itself involved in further thrusting (Improta et al., 2017; Mazzoli et al., 2008; Menardi Noguera & Rea, 2000; Patacca & Scandone, 2001). In particular, because of the subsequent extensional tectonic phases along the Apennine belt, the pre-existing thrusts and folds were systematically cut by high-angle normal faults (Schiattarella et al., 2003).

Although the role of strike-slip tectonics in the evolution of the Southern Apennines is strongly debated, according to some authors, Plio–Pleistocene sinistral strike-slip tectonics would have displaced this part of the Apennine belt (Catalano et al., 1993, 2004; Cinque et al., 1993; Knott & Turco, 1991; Milia et al., 2017; Monaco et al., 1998; Schiattarella et al., 1994; Turco et al., 1990; Van Dijk et al., 2000a).

From a kinematic point of view, the end of compressional tectonics and the subsequent onset of extensional tectonics occurred in the Middle Pleistocene, when flexural subsidence stopped and widespread uplift began (Cinque et al., 1993; Patacca & Scandone, 2007).

Currently, in this area active stress data (mainly from earthquakes, borehole breakouts, and faults; Fig. 1) indicate minimum horizontal stress directions perpendicular to the belt axis up to its eastern front (Mariucci et al., 2002; Pierdominici et al., 2011), as can be easily deduced from the numerous seismic events showing a prevalent extensional tectonic regime (Bello et al., 2022; Mariucci & Montone, 2020, 2022; Montone & Mariucci, 2016), which is discussed in greater detail below.

Beyond the Val d'Agri Basin, several Quaternary basins, such as the Vallo di Diano, Auletta, and Melandro-Pergola basins, characterise the area (Fig. 2). The Vallo di Diano and Auletta basins are

tectonic depressions that trend NW–NNW, both ca. 5–6 km wide, and are about 35 km and 20 km long, respectively, characterised by recent tectonic activity (Amicucci et al., 2008; Barchi et al., 2007; Bruno et al., 2010; Cello et al., 2003; Galli et al., 2006; Moro et al., 2007; Papanikolau & Roberts, 2007; Villani & Pierdominici, 2010).
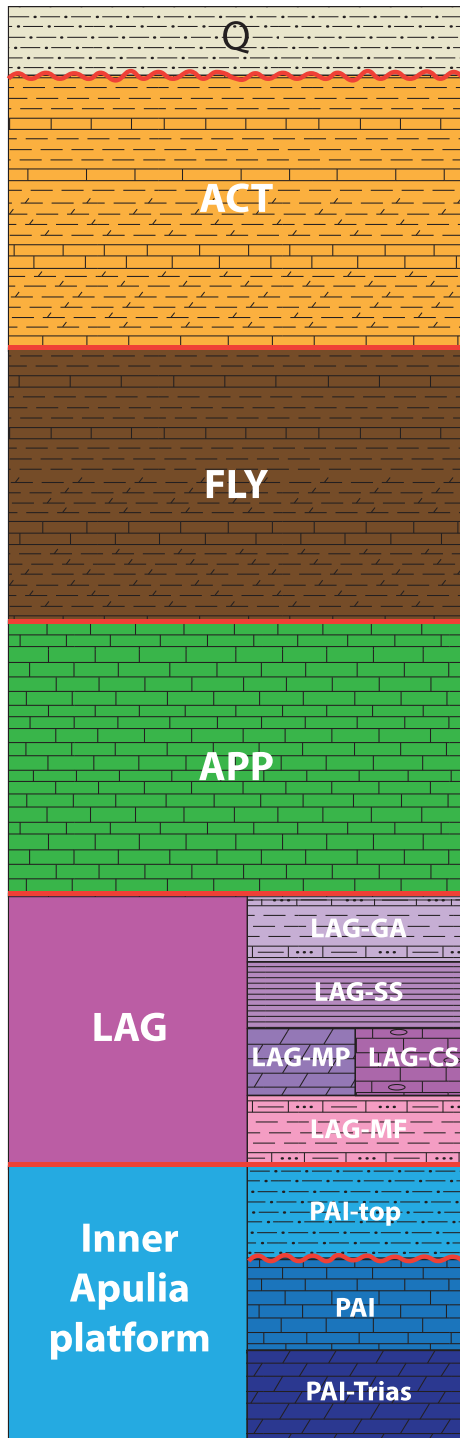
The Val d'Agri Basin contains the largest productive oil field in Europe; since the 1990s, hydrocarbons have been extracted from a highly productive reservoir consisting of Cretaceous limestones (Trice, 1999). This reservoir is hosted in large anticlines involving the Apulia platform, representing a natural structural trap of the oilfield. These anticlines are drilled at depths of 2 to 3 km below sea level and are sealed by flysch and mélange sequences (Improta et al., 2017; Nicolai & Gambini, 2007; Shiner et al., 2004). The Val d'Agri is a Quaternary extensional basin elongated about N120, approximately 30 km long and 5 km wide. The Quaternary sediments of the basin are entirely composed of Pleistocene continental clastic and alluvial sequences (Giano et al., 2000), which reach a thickness of about 250 m in the depocenter of the basin (Barchi et al., 2007).

The Val d'Agri Basin is bounded by two WNW-trending parallel and oppositely dipping high-angle normal fault systems (Cello et al., 2000; Improta et al., 2015). The eastern system is characterised by a set of NW–WNW transtensional faults dipping toward the SW (Cello et al., 2003), whereas the western system is mainly characterised by NE-dipping extensional faults, called the "Monti della Maddalena Extensional Fault System" (Maschio et al., 2005). According to Giano et al. (2000), these faults acted as left-lateral strike-slip structures during the Early Pleistocene and reactivated, mainly as normal faults, in the Middle Pleistocene–Holocene. In particular, the faults bordering the Agri basin are widely recognised as presently active (Benedetti et al., 1998; Cello et al., 2000; Valensise & Pantosti, 2001). According to some authors, based on different geological, geophysical, and geodetic data, the "Monti della Maddalena fault system" represents the main seismogenic structure of the region (Improta et al., 2010, 2015 and references therein; Ferranti et al., 2014).

As mentioned above, in this sector of the Apennines, NE-SW directed regional extension drives the activity of NW–SE-trending seismogenic structures (dipping either NE or SW), such as the fault associated with the M 6.9 1980 Irpinia earthquake and the Val d'Agri Basin faults (see also Westaway & Jackson, 1987; Pantosti & Valensise, 1990; Pantosti et al., 1993; Benedetti et al., 1998; Maschio et al., 2005; Basili et al., 2008), at least to the Calabria region (Fig. 1), where active extension gently rotates following the arcuate structure of the region (Cirillo et al., 2022; Mariucci & Montone, 2022). In fact, from a seismological perspective, instrumental data show that moderate to strong crustal earthquakes occurred under a prevalent extensional stress regime mostly concentrated along the Apennine belt. Some seismic events with lower magnitudes occurred along the adjacent foredeep. These events are characterised by greater crustal depths (ca. 40 km), and although the present-day extension is always oriented NE-SW, they show a prevalent strike-slip tectonic regime (Amato & Montone, 1997; Azzara et al., 1993; Barba et al., 2010; Ekstrom, 1994; Mariucci & Montone, 2022; Mariucci & Müller, 2003; Valensise et al., 2004), which suggests the existence of E–W right-lateral strike-slip faults dissecting the belt (Di Bucci et al., 2006; Scrocca et al., 2005). Historically (Rovida et al., 2020, 2022), this area was affected by destructive earthquakes with intensities up to XI, such as the M 7.1 earthquake that devastated the Val d'Agri Basin and a large area of Basilicata and part of Campania in 1857, revealing the high seismic hazard of this region. Apart from natural seismicity, induced seismicity has also been reported in the south-western sector of the Val d'Agri Basin (Improta et al., 2017; Lopez-Comino et al., 2021; Stabile et al., 2021) with a maximum magnitude Ml = 2 (Stabile et al., 2014), caused by wastewater reinjection operations in the disposal well of Costa Molina 2 (well 18).

2.1. Tectono-Stratigraphic Units

Considering the geographic location and stratigraphic similarity, we divided the wells into 9 groups assigning them different colours, as shown in Fig. 2. Then, we have analysed the stratigraphic log data of all wells and combined all the formations and

lithologies into tectono-stratigraphic units, as defined in Fig. 3.

We have taken into account the main geologic formations as well as the tectonic complexity of the Southern Apennines; therefore, Fig. 3 is not a stratigraphic column in the typical sense but a simple representation, not to scale, of the tectono-stratigraphic units used in this paper to examine the physical properties of the uppermost several kilometres of the crust. Because of the complex tectonic setting, in some areas, the stratigraphic succession is interrupted by tectonic contacts as outlined in Fig. 3.

The tectono-stratigraphic units have been divided into several sub-units where differences in the sonic record are clearly distinguishable. For example, in the Lagonegro unit, the five different formations that compose it are well identified. In contrast, where the sonic log is particularly variable and does not allow clear definition of individual units from each other, we have considered all the formations as a unique unit, such as the Tertiary flysch, for instance (Fig. 3).

The tectono-stratigraphic units are briefly described below (Fig. 3). We have divided the inner Apulia carbonate platform unit because of their specific characters easily recognisable from the sonic logs in: the Triassic succession (PAI-Trias), mainly dolostones; the calcareous-dolomitic Cretaceous-Miocene succession (PAI); and the clayey and arenaceous Pliocene succession (PAI-top), unconformably overlying the Apulia platform carbonates.

The middle Triassic–Cretaceous succession of the Lagonegro basin (LAG) is clearly represented in all the wells. It is composed of formations properly characterised by the sonic log and also recognised in the well composite logs. Therefore, for most of the analysed sonic length, a split analysis has been possible that has allowed the characterisation of each formation. The Monte Facito formation (LAG-MF) is characterised by a chaotic complex of terrigenous sediments and shallow-water carbonates of Middle Triassic age. The Calcari con Selce formation (LAG-CS), Late Triassic in age, is characterised by low-porosity multilayer carbonates, partially dolomitised and often nodular, with chert beds and nodules. In only one well (well 1), LAG-CS is substituted by dolostones of the Monte Pierno formation (LAG-MP) of the same age, Late Triassic. Deep-water facies characterise the Jurassic Scisti Silicei formation (LAG-SS), and the Galestri flysch formation (LAG-GA) comprises terrigenous deep-water facies of Late Jurassic–Early Cretaceous age.

The Apennine carbonate platform (APP) was encountered in only two wells (2 and 4), which are located NW outside of the Val d'Agri Basin (Fig. 2); this succession is characterised by calcareous dolomite deposits of the Triassic–Cretaceous.

The Tertiary flysch (FLY) mainly includes the Sicilidi, Liguridi, and Irpine deposits (Eocene–Miocene). All the flysch have been grouped for joint analysis because it is not possible to obtain reliable characteristic values for each one.

The Allochthonous succession (ACT) includes the Albidona and Gorgoglione flysch (Miocene). We have analysed this succession separately from the previous flysch formations (FLY) based on its tectonic position, although, as discussed below, the sonic logs and velocity values are similar.

Figure 3 also shows the Quaternary deposits for comparison with Fig. 2, even if no sonic log data are available, because these successions are limited to very thin thicknesses and drilled only in the shallower parts of the wells, where downhole logging typically is not performed.

3. Methods

We have analysed sonic log data from 28 deep oil wells, mainly located in the Val d'Agri Basin and surrounding areas. The analysis has been performed using original plots of 1:1000 scale (composite logs) because digital sonic records were not available to us.

The sonic tool records the full waveform travel times (slowness) of the high-frequency acoustic waves through the borehole from the emitters to the receivers. The slowness is used to infer the elastic wave velocities, providing good estimations despite the small volume investigated around the borehole (typically with a radius of a few tens of centimetres) and the different frequency from that of seismic waves (e.g. Ellis & Singer, 2008). This parameter varies depending on lithology, rock texture, and porosity, and thus provides information for the identification of lithologies, different compaction states, reservoir characteristics, and identification of the presence of fractures. Its main use is to supply information to support and calibrate seismic data and to estimate formation porosity (e.g. Ellis & Singer, 2008).

In the first few hundred metres, there is usually no sonic curve record. In those cases, to assign a reliable value we relied on the lithology and, where present, on the resistivity and gamma ray curves. In any case, these data were not considered for the calculation of the mean *Vp* of the single formations but only for the calculation of the overburden load. In particular, the resistivity allowed us to understand that in some cases the velocity variations were due to variations in porosity or alteration of the material encountered along the well and not to errors due to malfunctions of the instrument.

Throughout each well, we have identified depth ranges with uniform trend of sonic record, and assigned a slowness value (hand-picked with an accuracy/resolution of ± 2 μs/ft) with a quality rank to each interval. We have used three quality levels (good, medium, low), based on the feature of the sonic curve trend, to eventually discard some measurements and to use only the best data if necessary. In sedimentary rocks, measured slowness is typically between 40 and 140 μs/ft, reaching much higher values, up to 170 μs/ft, for example, in less
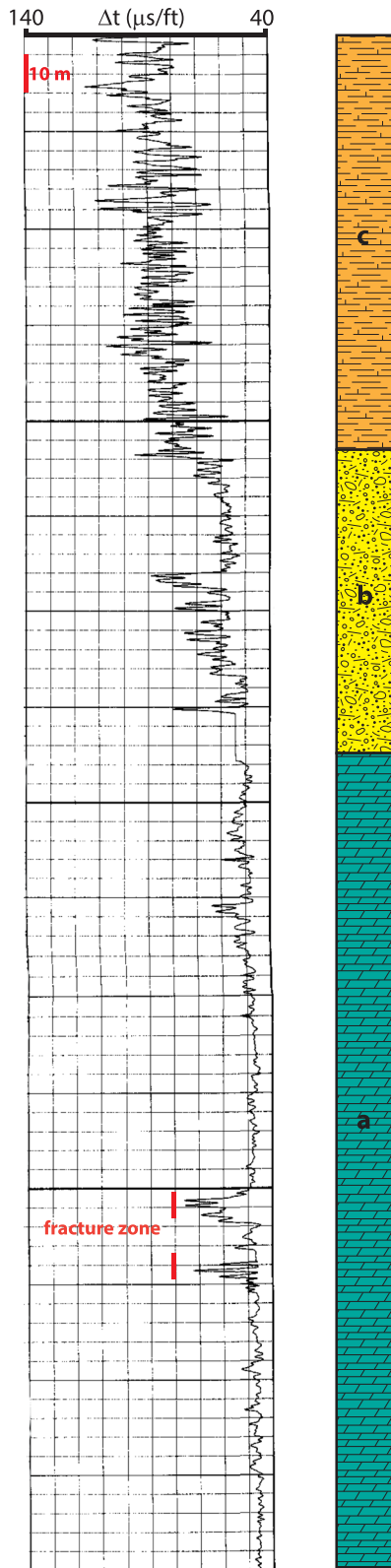
Example of a sonic tool record (Δt: transit time or slowness) from 40 to 140 μs/ft with respect to different lithologies and in the presence of a fracture zone. **a** Dolomite rock; **b** conglomerates; **c** clay and marls alternations

competent lithologies, such as Quaternary sediment (e.g. Ellis & Singer, 2008; Montone & Mariucci, 2015; Süss & Shaw, 2003). In the study area, the minimum and maximum values are 44 and 130 μs/ft, respectively. Each value has been then converted into P-wave velocity, ranging from 6.9 to 2.3 km/s relative to evaporitic and terrigenous formations, respectively.

Using the empirically derived formula by Gardner et al. (1974), that relates seismic P-wave velocity to the bulk density, we have estimated a density value for each homogeneous interval of the sonic record:

$$d = 0.23V^{0.25}$$

where d is density in g/cm^3 and V is sonic velocity in ft/s.

This rule provides good density predictions for sedimentary rocks, although using the Nafe–Drake curve (Ludwig et al., 1970) yields values about 0.1 g/cm^3 lower, according to Brocher (2005). Differently, Gardner's relation gives an inaccurate density value in zones where anhydrite is prevalent. For this reason and because anhydrites are present in very limited intervals along the analysed wells, we have not estimated the density value separately from the rest of the evaporitic succession.

It is difficult to precisely define an average velocity in formations characterised by thin alternations of different lithologies, such as clay and marls (Fig. 4); the different rock physical properties produce wide oscillations of slowness over small intervals of depth, as shown in the example of Fig. 4, providing a mean value with large uncertainty. In the presence of carbonate and dolomitic lithologies, the slowness value in the log can vary between 45 and 55 μs/feet (only 10 μs/feet of difference), depending on the presence of contamination or alteration, the chemical composition of the material, and/or fractured zones in the rock. In this case, because of unit conversion, the corresponding velocity values vary
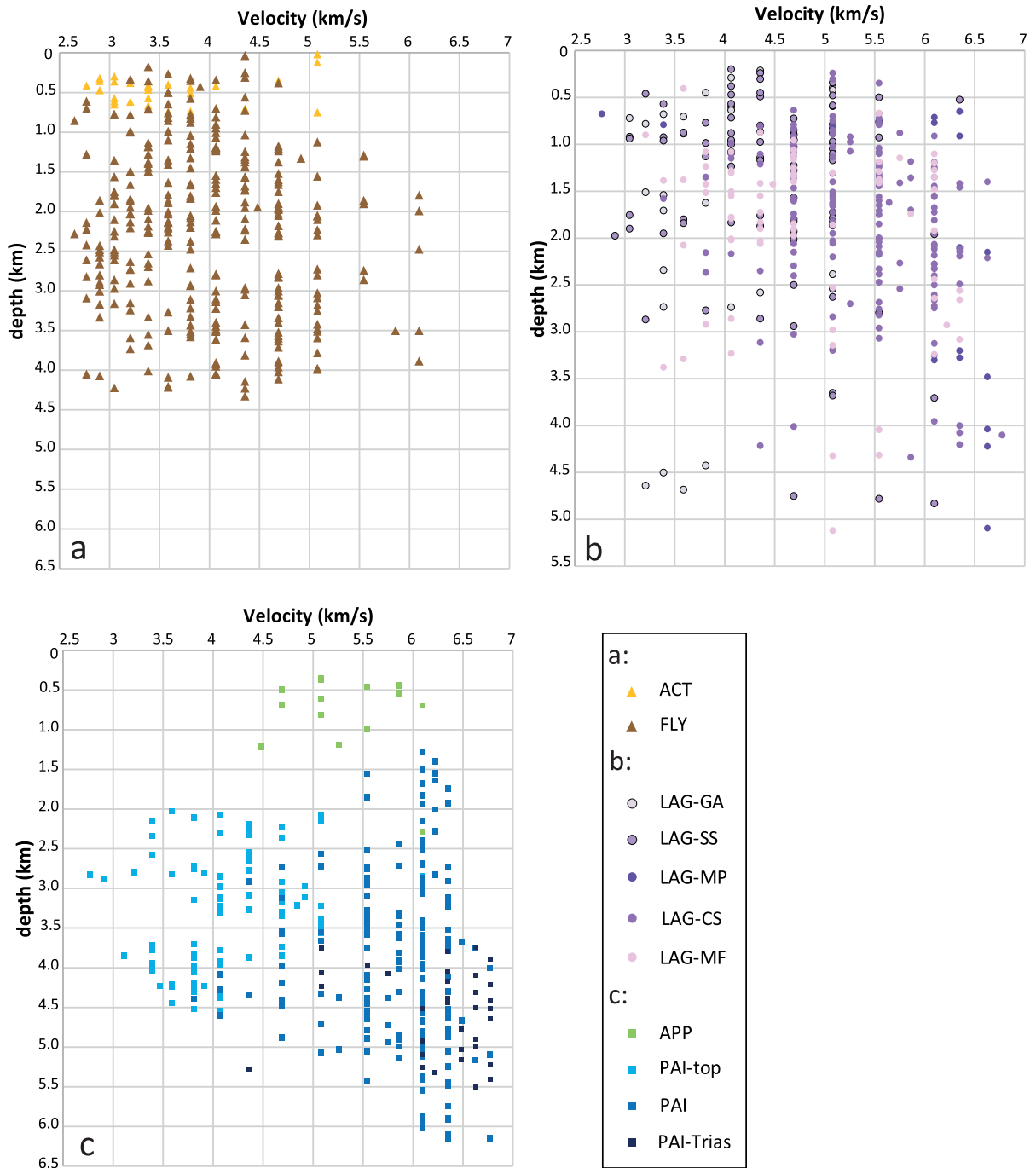
Figure 5

P-wave velocities versus depth for the 28 wells. **a** Allochthonous (ACT) and flysch (FLY) units. **b** Lagonegro units: LAG-GA, Galestri formation; LAG-SS, Scisti Silicei formation; LAG-MP, Monte Pierno formation; LAG-CS, Calcari con Selce formation; LAG-MF, Monte Facito formation. **c** Apennine carbonate platform (APP), and Inner Apulia successions: PAI-top, terrigenous deposits; PAI, carbonate succession; PAI-Trias, evaporitic succession. Depth refers to ground level

Table 1

P-wave velocities (km/s) of the main tectono-stratigraphic units compared with those reported in other studies

	This study		Other authors			
	1	2	3	4	5	6
ACT	3.3 (2.9–4.0)	3.5 ± 0.5			3.4–4.0[a]	
APP	5.9 (4.8–6.1)	5.7 ± 0.5			4.8–5.5[b]	
					4.5–5.8[c]	
FLY	3.7 (3.0–4.7)	3.9 ± 0.7	4.57 (3.59–3.48)[d]	3.0–4.0[e]	3.0–3.5[f]	3.0–4.0[h]
					3.8–5.0[g]	
LAG	5.0 (3.8–6.2)	5.1 ± 0.9	5.24 (4.43–6.34)	4.0–5.5		5.0–6.0[i]
GA	3.6 (3.2–4.9)	4.0 ± 0.6	4.74 (4.33–4.92)		3.4–3.7	
SS	4.3 (3.3–5.0)	4.4 ± 0.7	4.99 (4.31–5.42)			
MP	6.4 (5.7–6.6)	6.3 ± 0.7				
CS	5.4 (4.5–6.1)	5.5 ± 0.6	6.06 (4.93–6.55)			
MF	4.6 (3.8–6.1)	5.0 ± 0.9	4.76 (4.34–5.24)			
PAI-top	4.0 (3.3–4.9)	4.2 ± 0.6				
PAI	6.0 (5.5–6.3)	6.1 ± 0.4	6.29 (6.13–6.46)	5.8–6.0[l]	5.9–6.2	6.0–6.2
				6.5–6.6[m]		
PAI-Trias	6.5 (5.8–6.7)	6.4 ± 0.4		6.4–6.5	6.4–6.5	

1 Median value of the cumulative distribution by length and 10th–90th percentiles, *2* Mean weighted by length and standard deviation, *3* Pajola et al., (2020), *4* Improta et al., (2017), *5* Valoroso et al., (2011), *6* Valoroso et al., (2009). *ACT* Allochthonous succession (Miocene), *APP* Apennine carbonate platform (Late Trias-Cretaceous), *FLY* flysch units (mainly Eo-Miocene), *LAG* Lagonegro basin succession (Middle Triassic- Cretaceous): *GA* Galestri formation (Late Jurassic-Early Cretaceous), *SS* Scisti Silicei formation (Jurassic), *MP* Monte Pierno formation (Late Triassic), *CS* Calcari con selce formation (Late Triassic), *MF* Monte Facito formation (Middle Triassic), *PAI-top* Pliocene terrigenous deposits, *PAI* inner Apulia platform carbonate succession (Meso-Cenozoic), *PAI-Trias* Triassic evaporitic succession of the PAI. See text for a detailed description

[a]Flysch e thrust-sheet-top terrigenous deposits (Miocene–Pliocene)

[b]Mesozoic Limestones

[c]Cherts, cherty limestones, dolomites, siltstones

[d]Irpina-1, Irpina-2, Irpina-3

[e]Allochthonous nappes

[f]Paleogene variegated clays

[g]Paleogene Calcareous and arenaceous turbidites

[h]Shales and siliciclastic deposits

[i]Basinal and shelf carbonates

[l]Creta-Tertiary

[m]Jurassic-lower Cretaceous (dolomitic limestone and dolostones

quickly, changing from 6.8 to 5 km/s (almost 2 km/s of difference), whereas for lithologies with higher sonic values, the same Vp difference (about 2 km/s) corresponds to a larger slowness change. Therefore, the curve in non-digital logs for rocks with low values of slowness (corresponding to high Vp) must be read with great precision to avoid errors in Vp velocities. However, lithologies with low values of slowness typically show relatively little variability in the sonic record, whereas lithologies with high values of slowness are characterised by high variability.

By comparing stratigraphic and sonic logs, we have associated Vp and density data with units, as described in detail in the following section (see Fig. 3). The P-velocities versus depth for all the different tectono-stratigraphic units in the study area are shown in Fig. 5. Statistical analysis of all data within each unit has allowed the identification of average values for velocity and density, as well as their variability. The resulting values are listed in Table 1 and plotted in Fig. 6 as means by length and standard deviations, and as medians of the empirical
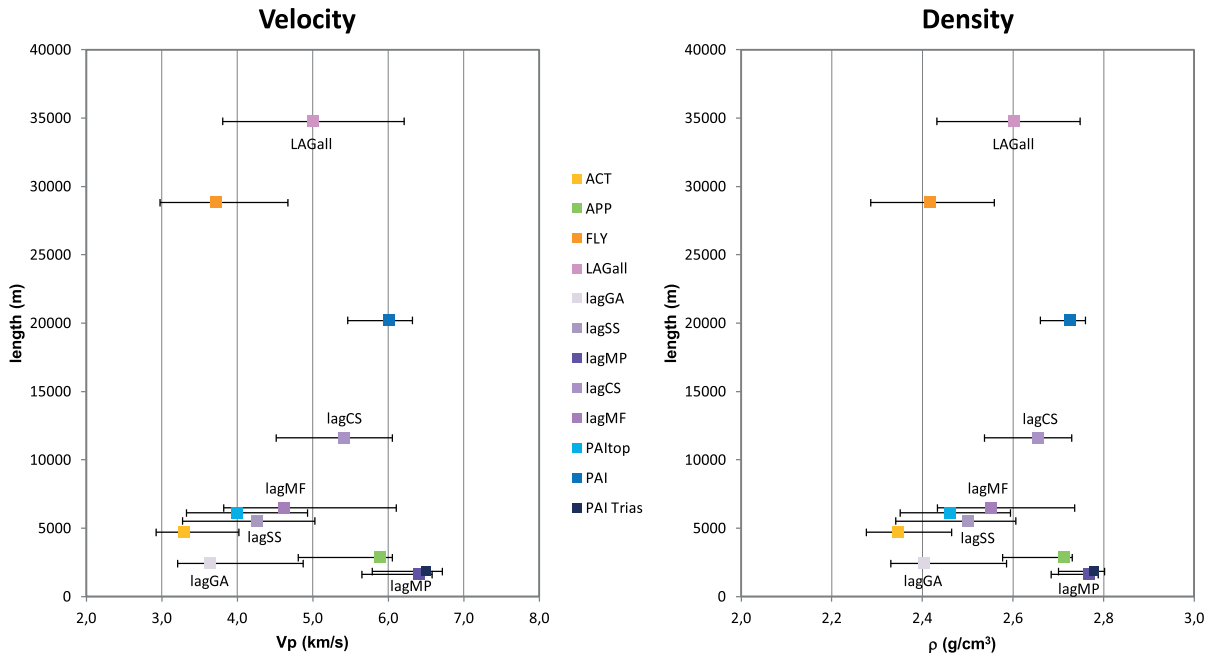
Figure 6
Sonic velocities and densities versus total analysed length for each tectono-stratigraphic unit. The central value is the median (50th percentile), and the range of natural variability is represented by the 10th and 90th percentiles
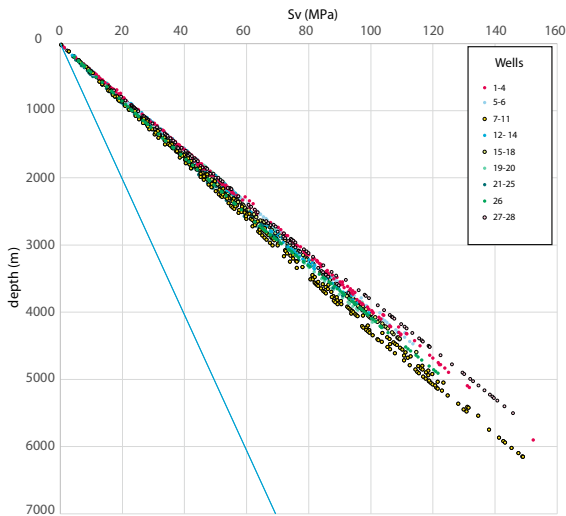

Figure 7
Vertical stress (*Sv*) magnitude versus depth in the 28 analysed wells (assembled following Fig. 2). Depth refers to ground level. Blue line indicates hydrostatic pressure. The lithostatic gradient ranges from ∼ 23 to ∼ 26 MPa/km

Velocity-derived densities have been used to compute the trend of the vertical stress magnitude with depth and to assess the limit values of the lithostatic gradient in the area (Fig. 7).

4. Results and Discussion

In this section, we refer to the average *Vp* and density values obtained in the analysis of the frequency distribution shown in Tables 1 and 2 (column 1). In the same tables, the mean values weighted by length and their standard deviations are also provided (column 2).

In a limited area, with maximum extents of 70 km in length by 35 km in width, we observed great variability in the *P*-wave velocity in relation to the formations crossed, within the same lithology and/or the tectono-stratigraphic unit itself, as well as with respect to depth (Fig. 5). From 0 to 4.5 km depth, we observe *P*-wave values ranging from 2.6 to 6.8 km/s; only below 5 km depth, the values of the *P*-waves are confined between 5.5 and 6.8 km/s. This large

cumulative distribution (50th percentile) and 10th–90th percentiles for the corresponding range of variability.

Table 2

Density values (g/cm³) of the main tectono-stratigraphic units

	1	2
ACT	2.35 (2.28–2.46)	2.38 ± 0.09
APP	2.71 (2.58–2.73)	2.69 ± 0.06
FLY	2.42 (2.29–2.56)	2.44 ± 0.11
LAG	2.60 (2.43–2.75)	2.61 ± 0.12
GA	2.40 (2.33–2.59)	2.45 ± 0.10
SS	2.50 (2.34–2.61)	2.52 ± 0.10
MP	2.77 (2.68–2.79)	2.76 ± 0.09
CS	2.66 (2.54–2.73)	2.66 ± 0.07
MF	2.55 (2.43–2.74)	2.59 ± 0.12
PAI-top	2.46 (2.35–2.59)	2.48 ± 0.09
PAI	2.73 (2.66–2.76)	2.73 ± 0.04
PAI-Trias	2.78 (2.70–2.80)	2.77 ± 0.05

ACT Allochthonous succession (Miocene), *APP* Apennine carbonate platform (Late Trias-Cretaceous), *FLY* flysch units (mainly Eo-Miocene), *LAG* Lagonegro basin succession (Middle Triassic-Cretaceous), *GA* Galestri formation (Late Jurassic-Early Cretaceous), *SS* Scisti Silicei formation (Jurassic), *MP* Monte Pierno formation (Late Triassic), *CS* Calcari con selce formation (Late Triassic), *MF* Monte Facito formation (Middle Triassic), *PAI-top* Pliocene terrigenous deposits, *PAI* inner Apulia platform carbonate succession (Meso-Cenozoic), *PAI-Trias* Triassic evaporitic succession of the PAI. See text for a detailed description, *1* median value of the cumulative distribution by length and 10th-90th percentiles, *2* mean weighted by length and standard deviation

variability is not observed, for example, in the northern or central Apennines, where a linear increase in velocity with increasing depth is more evident (Montone & Mariucci, 2015, 2020; Trippetta et al., 2021). This may be due not so much to the presence of a different stratigraphic succession, but probably to tectonics which in this region is more accentuated, with several compressive phases which have led to important shortening along the major thrusts.

In the compilation of previously published *P*-wave velocity data in the northern Italy area, for the Triassic dolomite succession, observed *Vp* values vary from 5 to ∼ 6.8 km/s, with a mean value of 6 km/s (Montone & Mariucci, 2015). Similarly, in the central Apennines, *Vp* in the Triassic evaporitic succession shows a mean value of 6.1 km/s (5.6–6.7) (Montone & Mariucci, 2020). These values are consistent with these new data for the dolostones that are present both in the Apulia platform Triassic

succession (PAI-Trias) and in the distinct formation (LAG-MP) of the Lagonegro basin succession, with slightly higher *Vp* values of 6.5 and 6.4 km/s, respectively (Fig. 5b, c). The same values have been found for the Triassic evaporites (dolostone and anhydrite) at the base of the inner Apulia platform using different kinds of data and methods: that is, passive seismic tomography of carbonate reservoirs (Bally et al., 1986; Improta et al., 2000, 2017; Tselentis et al., 2011; Valoroso et al., 2009, 2011). As in laboratory measurements, the *P*-velocity values for the dolomitic rocks are around 6.4–6.5 km/s (Trippetta et al., 2010).

We have analysed several wells that crossed the inner Apulia platform, for a total length of ∼ 20 km of the log record. The transition to the carbonate platform (Fig. 5c) is marked by a sudden jump in *P*-velocity from 4 to 6 km/s (Table 1), caused by the presence of a layer of one hundred metres of clayey rock (PAI-top). The PAI begins at a depth of 1250 m (below ground level) and extends to a depth of over 6000 m, with values between 5.5 and 6.5 km/s. This variability in the velocity values also exists because we did not subdivide the more dolomitic basal members (Jurassic–lower Cretaceous) from the remaining carbonate successions. Instead, the Apulia platform top (PAI-top) shows values between 3.5 and 5 km/s, with a mean *Vp* value of 4 km/s, and in some of the analysed wells, it was found at 2000 m minimum depth below ground level (Fig. 5c). An analysis recently performed along deep wells of the Val d'Agri Basin (Pajola et al., 2020), the carbonate platform (the whole Meso-Cenozoic succession) showed a *Vp* value of 6.3 km/s, consistent with what we observed (Table 1). Again, there is good agreement of our findings with the local earthquake tomography data (Improta et al., 2017; Valoroso et al., 2009, 2011).

The results obtained for the Apennine carbonate platform (APP) indicate great *Vp* variability, ranging between 4.8 and 6.1 km/s (Fig. 5c), with a median value of 5.9 km/s (Table 1). Results from passive tomography indicated *Vp* between 4.8 and 5.5 km/s (Valoroso et al., 2011).

The Lagonegro succession (LAG) is the most variable in terms of *Vp* (Fig. 5b): the average value is ∼ 5 km/s (Table 1), but the range varies between

3.2 and 6.6 km/s (Fig. 6). Within this succession we have found the highest value calculated in the analysis of these wells, corresponding to $Vp > 6.9$ km/s, sonic slowness at 44 μs/ft in the Calcari con Selce formation (LAG-CS), along well 26. The LAG was found between 0 and 5000 m deep. We have calculated the Vp value for each formation of this succession (Calcari con Selce, CS; Scisti Silicei, SS; Galestri, GA; Monte Pierno dolostone, MP; and Monte Facito, MF), and the results are more interesting and useful for detailed analysis (Fig. 5b). The analysis of Pajola et al. (2020) is in agreement with our results, suggesting a Vp value of 5.24 km/s (4.43–6.34 km/s) for the Lagonegro succession. The tomography results are also reported in Table 1, and although they refer to slightly different intervals, they are generally slightly lower than the values we have obtained.

The *P*-velocity values are lower in the terrigenous successions (ACT and FLY), ranging between ∼ 2.6 and ∼ 6.1 km/s (Fig. 5a). These data, above all, reveal the considerable variability of velocities associated with the presence of very different lithologies. Other authors (Table 1, column 5) aimed to identify different and more detailed lithostratigraphic units, and succeeded in identifying more precise values of velocity, although these results were affected by great uncertainty. In general, the borehole values appear to show systematically higher *P*-velocities.

The densities associated with all sedimentary lithologies show values that vary from a minimum of 2.3 g/cm^3 to a maximum of 2.8 g/cm^3 (Fig. 6). The highest values were found in the Triassic dolostones. In particular, this latter value is very well constrained, as shown by the associated small variability range, and estimated from a well-defined sonic record that reached values of 45 μs/ft. These high-density values refer to the dolomitic rocks found in wells at different depths (wells 5, 7, 9, and 28).

The maximum vertical stress (Sv) magnitude (Fig. 7), inferred from velocity-derived density values, is 152 MPa at 5900 m depth, computed for well number 2 in the Apennine carbonate platform (Fig. 2). A value of 26 MPa/km is confirmed for the lithostatic load in the Apennine belt *s.s.* (see Montone & Mariucci, 2015, 2020); the lithostatic gradient

varies between 23 MPa/km in the most external boreholes (toward the foredeep area) and 26 MPa/km in the southern boreholes, located along the belt (wells 27 and 28).

As highlighted by the results depicted in Fig. 5, in this area, it is difficult to identify a layered model with defined velocities as suggested by tomographic data (Valoroso et al., 2009), in which two different velocity layers were identified between 0 and 6 km depth. In our opinion, in relation to the rather variable velocity trend, identifying at shallow depth a constant velocity model might generate even larger errors in subsequent elaborations (such as epicentral calculations, focal mechanisms, and interpretations of seismic lines).

We have constructed contour maps of interpolated velocity values at different depths below sea level (Fig. 8). This is a first attempt to display Vp areal distribution and to consider our results in relation to those of other methods showing Vp trends at different depth slices. To create different surfaces, we have used the kriging method, one of the best known and widely used methods for this type of processing. Kriging is a geostatistical gridding method of interpolation based on a Gaussian process governed by prior covariances.

Given the non-homogeneous distribution of the wells, we have restricted the analysis area to wells 4 to 28, excluding wells 1, 2, and 3. The data distribution suggests that the zone with the highest resolution is the central and north-eastern sector of the Agri area from 0 to 3 km depth. The uneven coverage of our data allows us to define some main features of the area only in broad terms, and some structures imaged in the maps could be more an effect of the data distribution than of lateral velocity variations. Differences in the velocity trend can be observed at sea level (Fig. 8a) along the Agri Basin, in which high velocity areas (higher than 5.5 km/s) are opposed to low velocity areas (lower than 4 km/ s), following a trend that seems transverse to the NW main structure orientation, similar to the ENE-oriented faults (Fig. 8h). At 0.5 km depth (Fig. 8b) the velocity differences are less severe. However, for all depths analysed, a high velocity area is always observed with respect to well 28, where the Apulia carbonate platform outcrops and characterises the

entire well. At 1 km depth (Fig. 8c), a high velocity area (up to 6 km/s) is found between two low velocity zones (up to 3 km/s), following a N–S trend. A low velocity area is observed at 1.5 km depth along the central and north-eastern portions of the study area (Fig. 8d). The same low velocity feature is also observable at greater depths (Fig. 8f, g). At 3 km depth (Fig. 8g), *Vp* seems to change gradually from higher to lower values (from SW to NE), following the Apennine belt–foredeep structure.

Similar complexity was also observed associated with the deep structures by joint interpretation of the resistivity model and a 3D seismic tomographic model obtained from the inversion of passive seismic data (Balasco et al., 2021). Similar to the local earthquake tomography data, the lateral *Vp* changes detected at shallow depths were primarily related to variations in lithology (Improta et al., 2017). According to the same authors, within the inner Apulia platform, significant *Vp* and *Vp/Vs* changes were mainly driven by variations in both lithology and fracture density. Other aspects such as porosity and fluid content could also be considered to explain, within the same geological formations, the variability observed in the data.

5. Concluding Remarks

In the examined area, we have defined in-situ *Vp* and density values for all previously identified units (lithologies and formations) crossed by the wells, associating each value with a clear range of variability (Tables 1 and 2). The results show that large variability accompany this type of data.

The *P*-wave velocities from 0 to 6 km depth have values ranging from < 2.9 km/s to more than 6.8 km/s within the more competent calcareous and siliceous successions, showing great *P*-velocity natural variability over a distance of several tens of kilometres. The densities of the investigated rocks show values from slightly less than 2.3 g/cm^3 up to 2.8 g/cm^3; maximum values are found for the dolostones, which have a density of 2.82 g/cm^3. Based on these data, we have estimated that the lithostatic gradient in this area changes from $\sim$ 23 MPa/km for the easternmost boreholes to $\sim$ 26 MPa/km for the innermost wells.

Figure 8 ▶

Maps of *P*-wave velocity (km/s) trends obtained by interpolating well data using the kriging method at different depths below sea level: **a** 0 km, **b** 0.5 km, **c** 1 km, **d** 1.5 km, **e** 2 km, **f** 2.5 km, and **g** 3 km. White dashed lines indicate Quaternary deposits of the Val d'Agri Basin. Black circles with numbers represent the wells. On the bottom right corner: h) structural scheme showing the Quaternary extensional fault systems (red), main thrust faults (black lines with triangles), and other faults (simplified from Improta et al., 2017); green circle denotes well 18; green dashed line borders the Quaternary deposits of the Val d'Agri Basin. We have used the Surfer program v. 19 for kriging data

At 5 km depth, the overburden stress varies from $\sim$ 115 to $\sim$ 135 MPa from the foredeep to the belt; at the same depth along the Val d'Agri Basin, the stress magnitude is slightly greater than 120 MPa.

Although the data show large natural variability, especially for the geological formations characterised by different lithologies, these findings can be used with greater confidence to detail the upper shallow crust in this sector of southern Italy.

The variability of the values found, both *Vp* and density, is inherent in the lithological type crossed by the well. Where the geological formations are characterised by well-defined lithotypes and with consistent petrophysical characters, the sonic curve is also well defined, and reading along the log is easy and precise (Fig. 4). On the contrary, in areas with more complex lithostratigraphy, characterised by successions of different lithotypes over small intervals, the sonic record is irregular with numerous oscillations and peaks (Fig. 4). In this case, it is necessary to rely on the experience of the operator who identifies the measurement; an average value can be obtained, but it will be affected by a wide error.

As mentioned above, in carbonate and dolomitic lithologies, the slowness varies little, but very small changes correspond to high variations in velocity because of unit conversion. In contrast, for the lithologies with higher slowness values, the same *Vp* difference corresponds to much greater change in slowness.

The reasons strong lateral variations in *Vp* exist, in at least the uppermost kilometres of depth, are various, and could be attributed to a combination of different factors, such as lithology, topographic

Lateral Variations of *P*-Wave Velocity from Deep Borehole Data
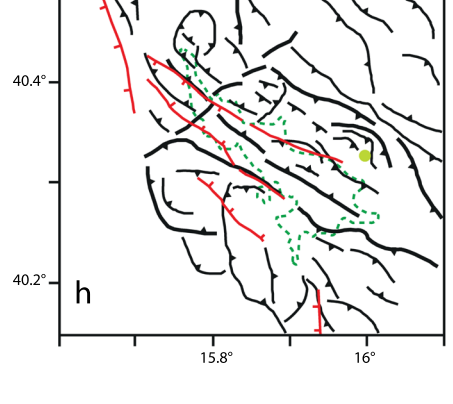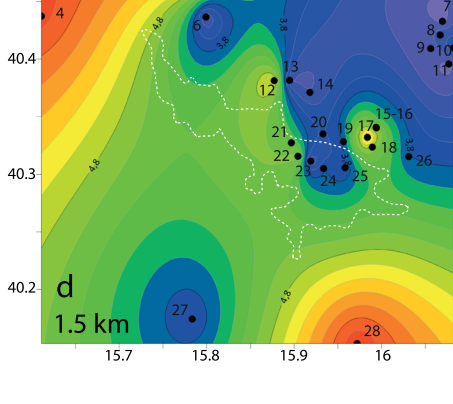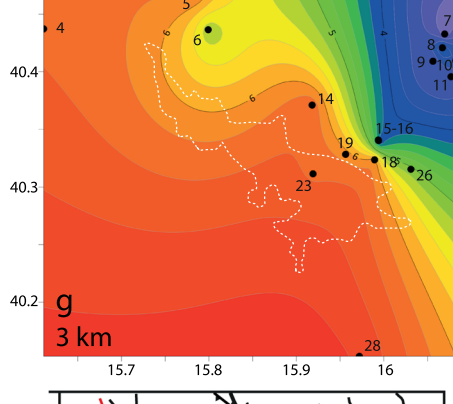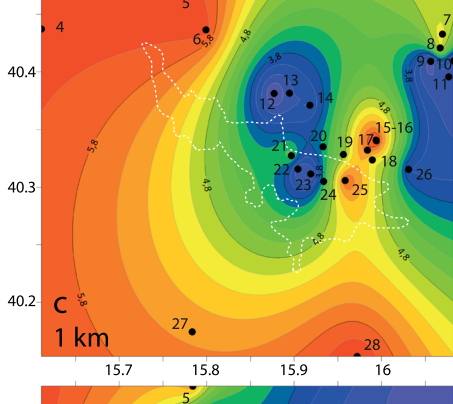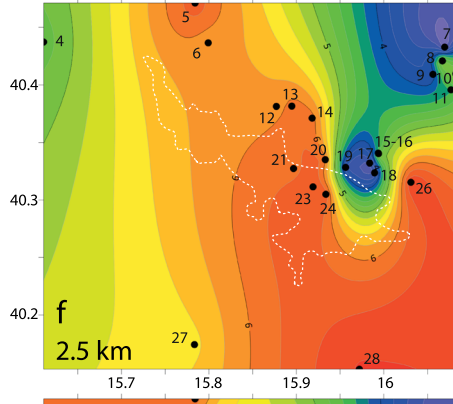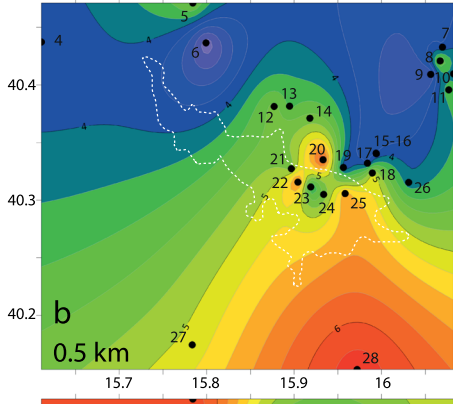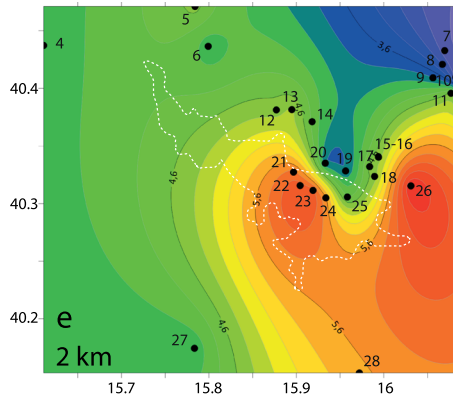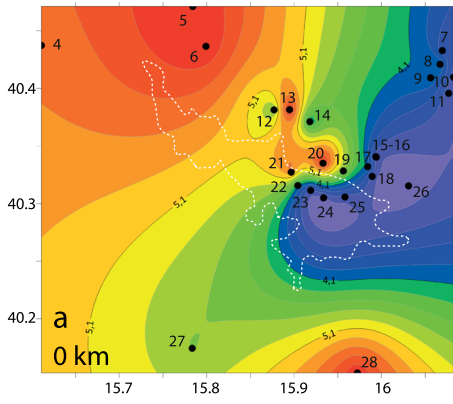
variation (linked to different heights above sea level of the wells), highly variable surface geology, and complex tectonics. For this last consideration, it should be noted that the Southern Apennine has undergone compressional tectonics with estimated shortening of 280–300 km (Scrocca et al., 2005), followed by superimposed extensional tectonics. Therefore, the important Vp variation both laterally and at depth are also the consequence of the juxtaposition of different paleogeographic domains, not allowing a linear velocity increase as is observed in other sectors of the Apennines. Furthermore, as stated by previous authors, in hydrocarbon reservoirs, several different factors can be considered to affect P-wave velocity; among these, lithology, porosity, fracture density, pore pressure, and fluid phase are the most important (Improta et al., 2017).

With this work we have aimed to define in detail the uppermost kilometres of crust that could be defined relatively poorly with other methods and that are normally neglected, to provide a contribution to better understand the correspondence between the main lithological units and seismic stratigraphy. From a geological point of view, knowledge of the correct P-wave velocities and the associated uncertainties will allow for accurate interpretation of seismic reflection profiles from the surface to deeper parts of the crust. With accurate depth conversion, we can then identify active tectonic structures that cut the Earth's surface. Understanding the uppermost kilometres of the crust can be considered the starting point for subsequent studies of seismic hazard.

Data availability

Data will be shared on request to the corresponding author with permission of ENI S.p.A. Part of sonic log data are available at https://www.videpi.com

Declarations

Conflict of interest The authors declare that they have no known competing financial interests or personal relationships that could have appeared to influence the work reported in this paper.

Publisher's Note Springer Nature remains neutral with regard to jurisdictional claims in published maps and institutional affiliations.

REFERENCES

Amato, A., & Montone, P. (1997). Present-day stress field and active tectonics in southern peninsular Italy. *Geophysical Journal International, 130*, 519–534.

Amato, A., et al. (1998). The Colfiorito, Umbria-Marche earthquake sequence in central Italy (Sept.-Nov., 1997): A first look to mainshocks and aftershocks. *Geophysical Research Letters, 25*, 2861–2864.

Amicucci, L., Barchi, M. R., Montone, P., & Rubiliani, N. (2008). The Vallo di Diano and Auletta extensional basins in the southern Apennines (Italy): A simple model for a complex

setting. *Terra Nova, 20*, 475–482. https://doi.org/10.1111/j.1365-3121.2008.00841.x

Azzara, R., Basili, A., Beranzoli, L., Chiarabba, C., Di Giovambattista, R., & Selvaggi, G. (1993). The seismic sequence of Potenza (May 1990). *Annali Di Geofisica, 36*(1), 237–243.

Balasco, M., Cavalcante, F., Romano, G., Serlenga, V., Siniscalchi, A., Stabile, T. A., & Lapenna, V. (2021). New insights into the High Agri Valley deep structure revealed by magnetotelluric imaging and seismic tomography (southern Apennine, Italy). *Tectonophysics, 808*, 228817. https://doi.org/10.1016/j.tecto.2021.228817

Bally, A. W., Burbi, L., Cooper, C., & Ghelardoni, R. (1986). Balanced cross-sections and seismic reflection profiles across the central Apennines. *Memorie Della Società Geologica Italiana, 35*, 257–310.

Barba, S., Carafa, M. M. C., Mariucci, M. T., Montone, P., & Pierdominici, S. (2010). Present-day stress-field modelling of southern Italy constrained by stress and GPS data. *Tectonophysics, 482*(1–4), 193–204. https://doi.org/10.1016/j.tecto.2009.10.017

Barchi, M. R., Amato, A., Cippitelli, G., Merlini, S., & Montone, P. (2007). Extensional tectonics and seismicity in the axial zone of the Southern Apennines. *Boll Society Geology Italy (italian Journal of Geoscience) Special Issue, 7*, 47–56.

Barchi, M. R., Carboni, F., Michele, M., Ercoli, M., Giorgetti, C., Porreca, M., Azzaro, S., & Chiaraluce, L. (2021). The influence of subsurface geology on the distribution of earthquakes during the 2016–2017 Central Italy seismic sequence. *Tectonophysics.* https://doi.org/10.1016/j.tecto.2021.228797

Basili, R., Valensise, G., Vannoli, P., Burrato, P., Fracassi, U., Mariano, S., Tiberti, M. M., & Boschi, E. (2008). The Database of Individual Seismogenic Sources (DISS), version 3: summarizing 20 years of research on Italy's earthquake geology. *Tectonophysics, 453*, 20–43.

Bello, S., Lavecchia, G., Andrenacci, C., Ercoli, M., Cirillo, D., Carboni, F., Barchi, M. R., & Brozzetti, F. (2022). Complex trans-ridge normal faults controlling large earthquakes. *Scientific Reports, 12*, 10676. https://doi.org/10.1038/s41598-022-14406-4

Benedetti, L., Tapponier, P., King, G. C. P., & Piccardi, L. (1998). Surface rupture of the 1857 southern Italian earthquake. *Terra Nova, 10*, 206–210.

Boncio, P., & Lavecchia, G. (2000). A geological model for the Colfiorito earthquakes (September-October 1997, central Italy). *Journal of Seismology, 4*(4), 345–356.

Brocher, T. M. (2005). Empirical relations between elastic wavespeeds and density in the earth's crust. *Bulletin Seismology Society of America, 95*(6), 2081–2092. https://doi.org/10.1785/0120050077

Bruno, P. P., Improta, L., Castiello, A., Villani, F., & Montone, P. (2010). The Vallo di Diano fault system: New evidence for an active range-bounding fault in southern Italy using shallow, high-resolution seismic profiling. *Bulletin of the Seismological Society of America, 100*(2), 882–890. https://doi.org/10.1785/0120090210

Buttinelli, M., Petracchini, L., Maesano, F. E., D'Ambrogi, C., Scrocca, D., Marino, M., Capotorti, F., Cavinato, G. P., Bigi, S., Mariucci, M. T., Montone, P., & Di Bucci, D. (2021). The impact of structural complexity, fault segmentation, and reactivation on seismotectonics: Constraints from the upper crust of the 2016–2018 central Italy seismic sequence area. *Tectonophysics, 810*, 228861. https://doi.org/10.1016/j.tecto.2021.228861

Calamita, F., Coltorti, M., Piccinini, D., Pierantoni, P. P., Pizzi, A., Ripepe, M., Scisciani, V., & Turco, E. (2000). Quaternary faults and seismicity in the Umbro-Marchean Apennines (Central Italy): Evidence from the 1997 Colfiorito earthquake. *Journal of Geodynamics, 29*(3–5), 245–264. https://doi.org/10.1016/S0264-3707(99)00054-X

Casero, P. (2004). Structural setting of petroleum exploration plays in Italy. In *Italian Geological Society for the IGC 32 Florence-2004, special volume* (pp. 189–199).

Catalano, S., Monaco, C., Tortorici, L., Paltrinieri, W., & Steel, N. (2004). Neogene-Quaternary tectonic evolution of the southern Apennines. *Tectonics, 23*, TC2003. https://doi.org/10.1029/2003TC001512

Catalano, S., Monaco, C., Tortorici, L., & Tansi, C. (1993). Pleistocene strike-slip tectonics in the Lucanian Apennine (southern Italy). *Tectonics, 12*(3), 656–665. https://doi.org/10.1029/92TC02251

Cello, G., Gambini, R., Mazzoli, S., Read, A., Tondi, E., & Zucconi, V. (2000). Fault zone characteristics and scaling properties of the Val d'Agri Fault System (Southern Apennines, Italy). *Journal of Geodynamics, 29*, 293–307.

Cello, G., Tondi, E., Micarelli, L., & Mattioni, L. (2003). Active tectonics and earthquake sources in the epicentral area of the 1857 Basilicata earthquake (southern Italy). *Journal of Geodynamics, 36*, 37–50. https://doi.org/10.1016/S0264-3707(03)00037-1

Chiarabba, C., & Amato, A. (2003). Vp and Vp/Vs images in the Mw 6.0 Colfiorito fault region (central Italy): a contribute to understand seismotectonic and seismogenic processes. *Journal of Geophysics Research, 108*, B5. https://doi.org/10.1029/2001JB001665

Chiaraluce, L., Di Stefano, R., Tinti, E., Scognamiglio, L., Michele, M., Casarotti, E., Cattaneo, M., De Gori, P., Chiarabba, C., Monachesi, G., Lombardi, A., Vaoloroso, L., Latorre, D., & Marzorati, S. (2017). The 2016 Central Italy seismic sequence: A first look at the mainshocks, aftershocks, and source models. *Seismological Research Letters, 88*(3), 757–771. https://doi.org/10.1785/0220160221

Cinque, A., Patacca, E., Scandone, P., & Tozzi, M. (1993). Quaternary kinematic evolution of the Southern Apennines Relationships between surface geological features and deep lithospheric structures. *Annals of Geophysics, 36*(2), 249–260. https://doi.org/10.4401/ag-4283

Cinti, F. R., Cucci, L., Marra, F., & Montone, P. (2000). The 1997 Umbria-Marche earthquakes (Italy): Relation between the surface tectonic breaks and the area of deformation. *Journal of Seismology, 4*, 333–343.

Cirillo, D., Totaro, C., Lavecchia, G., Orecchio, B., de Nardis, R., Presti, D., Ferrarini, F., Bello, S., & Brozzetti, F. (2022). Structural complexities and tectonic barriers controlling recent seismic activity in the Pollino area (Calabria–Lucania, southern Italy)—Constraints from stress inversion and 3D fault model building. *Solid Earth, 13*, 205–228. https://doi.org/10.5194/se-13-205-2022

Di Bucci, D., Ravaglia, A., Seno, S., Toscani, G., Fracassi, U., & Valensise, G. (2006). Seismotectonics of the southern Apennines and Adriatic foreland: Insights on active regional E-W shear zones from analogue modeling. *Tectonics, 25*, TC4015. https://doi.org/10.1029/2005TC001898

Di Stefano, R., Chiarabba, C., Chiaraluce, L., Cocco, M. D., Gori, P., Piccinini, D., & Valoroso, L. (2011). Fault zone properties

affecting the rupture evolution of the 2009 (Mw 6.1) L'Aquila earthquake (central Italy): Insights from seismic tomography. *Geophysics Research Letters, 38*, 10310. https://doi.org/10.1029/2011GL047365

Doglioni, C., Harabaglia, P., Martinelli, G., Mongelli, G., & Zito, G. (1996). A geodynamic model of the Southern Apennines accretionary prism. *Terra Nova, 8*, 540–547.

Ekström, G. (1994). Teleseismic analysis of the 1990 and 1991 earthquakes near Potenza. *Annali Di Geofisica, 37*, 1591–1599.

Ekström, E., Morelli, A., Boschi, E., & Dziewonski, A. M. (1998). Moment tensor analysis of the Central Italy earthquake sequence of September-October 1997. *Geophysical Research Letters, 25*, 1971–1974.

Ellis, D. V., & Singer, J. M. (2008). *Well logging for earth scientists* (2nd ed.). Springer.

Ferranti, L., Palano, M., Cannavò, F., Mazzella, M. E., Oldow, J. S., Gueguen, E., Mattia, M., & Monaco, C. (2014). Rates of geodetic deformation across active faults in southern Italy. *Tectonophysics, 621*, 101–122. https://doi.org/10.1016/j.tecto.2014.02.007

Galli, P., Bosi, V., Piscitelli, S., Giocoli, A., & Scionti, V. (2006). Late Holocene earthquakes in southern Apennine; Paleoseismology of the Caggiano fault. *Geologische Rundschau, 95*(5), 855–870.

Gardner, G. H. F., Gardner, L. W., & Gregory, A. R. (1974). Formation velocity and density: The diagnostic basics for stratigraphic traps. *Geophysics, 39*, 770–780.

Giano, S., Maschio, L., Alessio, M., Ferranti, L., Improta, L., & Schiattarella, M. (2000). Radiocarbon dating of active faulting in the High Agri Valley, southern Italy. *Journal of Geodynamics, 29*, 371–386.

Improta, L., Bagh, S., De Gori, P., Valoroso, L., Pastori, M., Piccinini, D., Chiarabba, C., Anselmi, M., & Buttinelli, M. (2017). Reservoir structure and wastewater-induced seismicity at the Val d'Agri Oilfield (Italy) shown by three-dimensional Vp and Vp/Vs local earthquake tomography. *Journal of Geophysical Research, 122*, 9050–9082. https://doi.org/10.1002/2017JB014725

Improta, L., Ferranti, L., De Martini, P. M., et al. (2010). Detecting young, slow-slipping active faults by geologic and multidisciplinary high-resolution geophysical investigations: A case study from the Apennine seismic belt, Italy. *Journal of Geophysics Research, 115*, B11307. https://doi.org/10.1029/2010JB000871

Improta, L., Iannaccone, G., Capuano, P., Zollo, A., & Scandone, P. (2000). Inferences on the upper crustal structure of the southern Apennines (Italy) from seismic refraction investigations and subsurface data. *Tectonophysics, 317*(3–4), 273–298. https://doi.org/10.1016/S0040-1951(99)00267-X

Improta, L., Valoroso, L., Piccinini, D., & Chiarabba, C. (2015). A detailed analysis of wastewater-induced seismicity in the Val d'Agri oil field (Italy). *Geophysical Research Letters, 42*, 2682–2690. https://doi.org/10.1002/2015GL063369

López-Comino, J. Á., Braun, T., Dahm, T., Cesca, S., & Danesi, S. (2021). On the source parameters and genesis of the 2017, Mw 4 Montesano earthquake in the outer border of the Val d'Agri Oilfield (Italy). *Frontiers Earth Science, 8*, 617794. https://doi.org/10.3389/feart.2020.617794

Ludwig, W. J., Nafe, J. E., & Drake, C. L. (1970). Seismic Refraction. In A. E. Maxwell (Ed.), *The sea* (Vol. 4, pp. 53–84). Wiley.

Knott, S. D., & Turco, E. (1991). Late Cenozoic kinematics of the Calabrian Arc, Southern Italy. *Tectonics, 10*(6), 1164–1172.

Mariucci, M. T., Amato, A., Gambini, R., Giorgioni, M., & Montone, P. (2002). Along-depth stress rotations and active faults: An example in a 5-km deep well of Southern Italy. *Tectonics, 21*(4), 1021. https://doi.org/10.1029/2001TC001338

Mariucci, M. T., & Müller, B. (2003). The tectonic regime in Italy inferred from borehole breakout data. *Tectonophysics, 361*, 21–35. https://doi.org/10.1016/S0040-1951(02)00536-X

Mariucci, M. T., & Montone, P. (2016). Contemporary stress field in the area of the 2016 Amatrice seismic sequence (central Italy). *Annals of Geophysics*. https://doi.org/10.4401/ag-7235

Mariucci, M. T., & Montone, P. (2020). Database of Italian present-day stress indicators, IPSI 1.4. *Scientific Data, 7*, 298. https://doi.org/10.1038/s41597-020-00640-w

Mariucci, M. T., & Montone, P. (2022). *IPSI 1.5, Database of Italian present-day stress indicators*. Istituto Nazionale di Geofisica e Vulcanologia (INGV). https://doi.org/10.6092/INGV.IT-IPSI.1.5.

Maschio, L., Ferranti, L., & Burrato, P. (2005). Active extension in Val d Agri area, southern Apennines, Italy: Implications for the geometry of the seismogenic belt. *Geophysical Journal International, 162*, 591–609. https://doi.org/10.1111/j.1365-246X.2005.02597.x

Mazzoli, S., D'Errico, M., Aldega, L., Corrado, S., Invernizzi, C., Shiner, P., & Zattin, M. (2008). Tectonic burial and "young" (<10 Ma) exhumation in the southern Apennines fold-and-thrust belt (Italy). *Geology, 36*(3), 243–246. https://doi.org/10.1130/G24344A.1

Mazzoli, S., Invernizzi, C., Marchegiani, L., Mattioni, L., & Cello, G. (2004). Brittle-ductile shear zone evolution and fault initiation in limestones, Monte Cugnone (Lucania), southern Apennines, Italy. *Geological Society, Special Publications, 224*, 353–373. https://doi.org/10.1144/GSL.SP.2004.224.01.22

Menardi Noguera, A., & Rea, G. (2000). Deep structure of the Campanian-Lucanian Arc, Southern Apennine, Italy. *Tectonophysics, 324*(4), 239–265. https://doi.org/10.1016/S0040-1951(00)00137-2

Milia, A., Torrente, M. M., & Iannace, P. (2017). Pliocene-Quaternary orogenic systems in Central Mediterranean: The Apulia-Southern Apennines-Tyrrhenian Sea example. *Tectonics, 36*, 1614–1632. https://doi.org/10.1002/2017TC004571

Monaco, C., Tortorici, L., & Paltrinieri, W. (1998). Structural evolution of the Lucanian Apennines Southern Italy. *Journal of Structural Geology, 20*(5), 617–638.

Montone, P., & Mariucci, M. T. (2015). P-wave velocity, density, and vertical stress magnitude along the crustal Po Plain (Northern Italy) from sonic log drilling data. *Pure and Applied Geophysics, 172*, 1547–1561. https://doi.org/10.1007/s00024-014-1022-5

Montone, P., & Mariucci, M. T. (2016). The new release of the Italian contemporary stress map. *Geophysical Journal International, 205*, 1525–1531. https://doi.org/10.1093/gji/ggw100

Montone, P., & Mariucci, M. T. (2020). Constraints on the structure of the shallow crust in central Italy from geophysical log data. *Scientific Reports, 10*(1), 3834. https://doi.org/10.1038/s41598-020-60855-0

Moro, M., Amicucci, L., Cinti, F. R., Doumaz, F., Montone, P., Pierdominici, S., Saroli, M., Stramondo, S., & Di Fiore, B. (2007). Surface evidence of active tectonics along the Pergola-Melandro fault: A critical issue for the seismogenic potential of

the southern Apennines, Italy. *Journal of Geodynamics, 44*(1–2), 19–32. https://doi.org/10.1016/j.jog.2006.12.003

Nicolai, C., & Gambini, R. (2007). Structural architecture of the Adria platform-and-basin system. In A. Mazzotti, E. Patacca, P. Scandone (Eds.) *Results of the CROP project, sub-project CROP-04 Southern Apennines (Italy). Italian Journal of Geoscience, 7,* 21–37.

Pajola, N., Pugliese, A., Toniolatti, L., Rubiliani, N., Borrini, D., Storer, P., Follino, P., & Perrone, L. (2020). Geologically driven seismic reprocessing: The Val d'Agri case history. *Bollettino Di Geofisica Teorica Ed Applicata, 61*(3), 273–292. https://doi.org/10.4430/bgta0310

Pantosti, D., Schwartz, D. P., & Valensise, G. (1993). Paleoseismology along the 1980 Irpinia earthquake fault and implications for earthquake recurrence in the southern Apennines. *Journal of Geophysical Research, 98,* 6561–6577.

Pantosti, D., & Valensise, G. (1990). Faulting mechanism and complexity of the November 23, (1980), Campania-Lucania earthquake, inferred from surface observations. *Journal of Geophysical Research, 95*(15), 319–341.

Papanikolau, I., & Roberts, G. (2007). Geometry, kinematics and deformation rates along the active normal fault system in the southern Apennines: Implication for fault growth. *Journal of Structural Geology, 29*(1), 166–188. https://doi.org/10.1016/j.jsg.2006.07.009

Patacca, E., & Scandone, P. (1989). Post-Tortonian mountain building in the Apennines. The role of the passive sinking of a relic lithospheric slab. In A. Boriani, M. Bonafede, G.B. Piccardo, G.B. Vai (Eds.), *The lithosphere in Italy* (vol. 80, pp. 157–176). Accademia Nazionale dei Lincei.

Patacca, E., & Scandone, P. (2001). Late thrust propagation and sedimentary response in the thrust belt- foredeep system of the Southern Apennines (Pliocene-Pleistocene). In G. B. Vai & I. P. Martini (Eds.), *Anatomy of a mountain: The Apennines and adjacent Mediterranean basins* (pp. 401–440). Kluwer Academic Publ.

Patacca, E., & Scandone, P. (2004). The Plio-Pleistocene thrust belt-foredeep system in the Southern Apennines and Sicily (Southern Apenninic Arc, Italy). *Italian Geological Society for the IGC 32 Florence-2004, Special Volume* (pp. 93–129).

Patacca, E., & Scandone, P. (2007). Geology of the Southern Apennines. *Bollettino Della Società Geologica Italiana (italian Journal of Geoscience) Special Issue, 7,* 75–119.

Pierdominici, S., Mariucci, M. T., & Montone, P. (2011). A study to constrain the geometry of an active fault in southern Italy through borehole breakouts and downhole logs. *Journal of Geodynamics, 52*(3–4), 279–289. https://doi.org/10.1016/j.jog.2011.02.006

Royden, L. E., Patacca, E., & Scandone, P. (1987). Segmentation and configuration of subducted lithosphere in Italy: An important control on thrust-belt and foredeep-basin evolution. *Geology, 15,* 714–717.

Roure, F., Casero, P., & Addoum, B. (2012). Alpine inversion of the North African margin and delamination of its continental lithosphere. *Tectonics, 31,* 3006. https://doi.org/10.1029/2011TC002989

Rovida, A., Locati, M., Camassi, R., Lolli, B., & Gasperini, P. (2020). The Italian earthquake catalogue CPTI15. *Bulletin of Earthquake Engineering, 18*(7), 2953–2984. https://doi.org/10.1007/s10518-020-00818-y

Rovida, A., Locati, M., Camassi, R., Lolli, B., Gasperini, P., & Antonucci, A. (2022). *Italian Parametric Earthquake Catalogue (CPTI15), version 4.0.* Istituto Nazionale di Geofisica e Vulcanologia (INGV). https://doi.org/10.13127/CPTI/CPTI15.4.

Schiattarella, M., Di Leo, P., Beneduce, P., & Giano, S. I. (2003). Quaternary uplift vs tectonic loading: A case study from the Lucanian Apennine, southern Italy. *Quaternary International, 101–102,* 239–251.

Schiattarella, M., Torrente, M. M., & Russo, F. (1994) Analisi strutturale ed osservazioni morfotettoniche nel bacino del Mercure (Confine calabro lucano). *Quaternario 7,* 613–626.

Scrocca, D., Carminati, E., & Doglioni, C. (2005). Deep structure of the southern Apennines, Italy: Thin-skinned or thick-skinned? *Tectonics, 24,* 3005. https://doi.org/10.1029/2004TC001634

Shiner, P., Beccaccini, A., & Mazzoli, S. (2004). Thin-skinned versus thick-skinned structural models for Apulian carbonate reservoirs: Constraints from the Val d'Agri Fields, S Apennines, Italy. *Marine Petroleum Geology, 21,* 805–827. https://doi.org/10.1016/j.marpetgeo.2003.11.020

Stabile, T. A., Giocoli, A., Perrone, A., Piscitelli, S., & Lapenna, V. (2014). Fluid injection induced seismicity reveals a NE dipping fault in the southeastern sector of the High Agri Valley (southern Italy). *Geophysical Research Letters, 41,* 5847–5854. https://doi.org/10.1002/2014GL060948

Stabile, T. A., Vlček, J., Wcisło, M., & Serlenga, V. (2021). Analysis of the 2016–2018 fluid-injection induced seismicity in the High Agri Valley (Southern Italy) from improved detections using template matching. *Scientific Reports, 11,* 20630. https://doi.org/10.1038/s41598-021-00047-6

Süss, P., & Shaw, J. H. (2003). Pwave seismic velocity structure derived from sonic logs and industry reflection data in the Los Angeles basin, California. *Journal of Geophysical Research, 108*(B3), 2170. https://doi.org/10.1029/2001JB001628

Tinti, E., Scognamiglio, L., Michelini, A., & Cocco, M. (2016). Slip heterogeneity and directivity of the ML 6.0 2016 Amatrice earthquake estimated with rapid finite-fault inversion. *Geophysics Research Letters, 43*(10), 745–752. https://doi.org/10.1002/2016GL071263

Trice, R. (1999). Application of borehole image logs in constructing 3D static models of productive fracture network in the Apulian platform. *Geological Society, Special Publications, 159,* 156–176. https://doi.org/10.1144/GSL.SP.1999.159.01.08

Trippetta, F., Barchi, M. R., Tinti, E., Volpe, G., Rosset, G., & De Paola, N. (2021). Lithological and stress anisotropy control large-scale seismic velocity variations in tight carbonates. *Scientific Reports, 11,* 9472. https://doi.org/10.1038/s41598-021-89019-4

Trippetta, F., Collettini, C., Vinciguerra, S., & Meredith, P. G. (2010). Laboratory measurements of the physical properties of Triassic Evaporites from Central Italy and correlation with geophysical data. *Tectonophysics, 492*(1–4), 121–132. https://doi.org/10.1016/j.tecto.2010.06.001

Tselentis, G. A., Martakis, N., Paraskevopoulos, P., Sokos, E., & Lois, A. (2011). High-resolution passive seismic tomography (PST) for 3D velocity, Poisson's ratio ν, and P-wave quality QP in the Delvina hydrocarbon field, southern Albania. *Geophysics, 76*(3), B1–B24. https://doi.org/10.1190/1.3560016

Turco, E., Maresca, R., & Cappadonna, P. (1990). La tettonica pliopleistocenica del confine calabro-lucano: Modello cinematico. *Memorie Della Societa'geologica Italiana, 45,* 519–529.

Valensise, G., & Pantosti, D. (2001). The investigation of potential earthquake sources in peninsular Italy: A review. *Journal of Seismology, 5*, 287–306.

Valensise, G., Pantosti, D., & Basili, R. (2004). Seismology and tectonic setting of the 2002 Molise, Italy, Earthquake 2002. *Earthquake Spectra, 20*, 23–37. https://doi.org/10.1193/1.1756136

Valoroso, L., Improta, L., Chiaraluce, L., Di Stefano, R., Ferranti, L., Govoni, A., & Chiarabba, C. (2009). Active faults and induced seismicity in the Val d'Agri area (Southern Apennines, Italy). *Geophysical Journal International, 178*, 488–502. https://doi.org/10.1111/j.1365-246X.2009.04166.x

Valoroso, L., Improta, L., De Gori, P., & Chiarabba, C. (2011). Upper crustal structure, seismicity and pore pressure variations in an extensional seismic belt through 3-D and 4-D VP and VP/VS models: The example of the Val d'Agri area (southern Italy). *Journal of Geophysical Research, 116*, B07303. https://doi.org/10.1029/2010JB007661

Van Dijk, J. P., Bello, M., Brancaleoni, G. P., Cantarella, G., Costa, V., Frixa, A., Golfetto, F., Merlini, S., Riva, M., Torricelli, S., Toscano, C., & Zerilli, A. (2000a). A regional structural model for the northern sector of the Calabrian Arc (southern Italy). *Tectonophysics, 324*, 267–320.

Van Dijk, J. P., Bello, M., Toscano, C., Bersani, A., & Nardon, S. (2000b). Tectonic model and three-dimensional fracture network analysis of Monte Alpi (southern Apennines). *Tectonophysics, 324*(4), 203–237.

Vezzani, L., Festa, A., & Ghisetti, F. C. (2010). Geology and tectonic evolution of the Central-Southern Apennines, Italy. *Special Paper Geology Society America, 469*, 1–58. https://doi.org/10.1130/2010.2469

Villani, F., & Pierdominici, S. (2010). Late Quaternary tectonics of the Vallo di Diano basin (southern Apennines, Italy). *Quaternary Science Reviews, 29*, 3167–3183. https://doi.org/10.1016/j.quascirev.2010.07.003

Walters, R. J., Elliott, J. R., D'agostino, N., England, P. C., Hunstad, I., Jackson, J. A., Parsons, B., Phillips, R. J., & Roberts, G. (2009). The 2009 L'Aquila earthquake (central Italy): A source mechanism and implications for seismic hazard. *Geophysical Research Letters, 36*(17)

Westaway, R., & Jackson, J. (1987). The earthquake of 1980 November 23 in Campania-Basilicata (southern Italy). *Geophysics Journal of Astronomy Society, 90*, 375–443.